

# Kinetics and Mechanism of Thiolytic Cleavage of the Antitumor Compound 4'-[(9-Acridinyl)amino]methanesulfon-*m*-anisidide

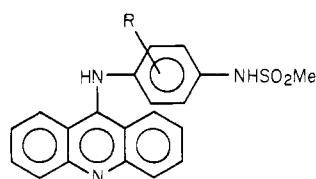
M. Niyaz Khan\* and L. Malspeis†

Department of Chemistry, Bayero University, Kano, Nigeria

Received December 7, 1981

The thiolysis of 4'-[(9-acridinyl)amino]methanesulfon-*m*-anisidide (*m*-AMSA) has been studied in buffer solutions of L-cysteine, glutathione, *N*-acetylcysteine, 2-mercaptoethanol, and cysteamine at various pH values. The thiolysis is sensitive to general-acid catalysis. Both free and protonated forms of *m*-AMSA have been found to be reactive for thiolysis. The Brønsted-type correlation of thiol basicity to the nucleophilic rate constants with the protonated *m*-AMSA (*m*-AMSA<sup>+</sup>H) has a slope,  $\beta_{\text{nuc}}$ , of  $0.74 \pm 0.07$  which indicates that probably the expulsion of the leaving group is the rate-determining step. The rate constants for general-acid-catalyzed thiolytic cleavage of *m*-AMSA<sup>+</sup>H reveal an insensitiveness to the acidity of catalysts. The general-acid-catalyzed rate constants for thiolysis of the free base of *m*-AMSA have been found to have quite high sensitivities to the  $\text{p}K_a$  of catalysts ( $\alpha = 0.57 \pm 0.07$ ) which has been interpreted by assuming a concerted type of mechanism for thiolysis. The various ionic forms of amino thiols are acting as nucleophiles as well as general-acid catalysts, depending upon the pH range of the reaction and the microscopic ionization constants of the thiols. The unionized thiol groups of most of the catalysts are acting as general acids except for cysteamine where the protonated amino group is also acting as a general-acid catalyst. A high nucleophilic rate constant for cysteamine with *m*-AMSA (free base) compared with those for other nucleophiles of similar basicity has been attributed to its probable ability of acting as an intramolecular general-acid catalyst. The thiolytic cleavage of *m*-AMSA<sup>+</sup>H is nearly  $10^3$  times faster than that of *m*-AMSA (free base) while the ratios for general-acid-catalyzed rate constants for *m*-AMSA<sup>+</sup>H and *m*-AMSA (free base) vary from 20 to 300 depending upon the  $\text{p}K_a$  of the catalysts. The bimolecular nucleophilic rate constant (with *m*-AMSA<sup>+</sup>H) as well as the general-acid-catalyzed rate constant (with *m*-AMSA free base) for glutathione is found to be positively deviated from Brønsted plots which seem as if they fall on a separate Brønsted plot of essentially the same slope but with a different intercept.

Recently, Cain and his co-workers<sup>1</sup> have tested a large number of acridine derivatives for antitumor activity, and it has been observed that 4'-[(9-acridinyl)amino]methanesulfon-*m*-anisidide (*m*-AMSA) is highly active toward



*m*-AMSA, R = 3'-OMe  
*o*-AMSA, R = 2'-OMe

certain types of cancerous cells while 4'-[(9-acridinyl)amino]methanesulfon-*o*-anisidide (*o*-AMSA) has shown no activity at all toward the same types of cancerous cells. In fact, *m*-AMSA is under clinical trial under the auspices of the Drug and Research Development Program, Division of Cancer Treatment, NCI.

Cain and his co-workers<sup>2</sup> have determined the half-life periods ( $t_{1/2}$ ) for thiolytic degradation of various acridine derivatives using 2-mercaptoethanol in phosphate buffer and tried to find a correlation between  $t_{1/2}$  and  $\text{p}K_a$  of acridine derivatives. Without realizing the complexity of the thiolytic degradation of these derivatives, these authors have used the apparent observed pseudo-first-order rate constants in modelling the dose potency of these drugs. 2-Mercaptoethanol, being a monofunctional catalyst, is considered to be a simpler thiol compared with cysteine and glutathione, which are polyfunctional catalysts, in correlating their *in vitro* and *in vivo* reactivities with a drug compound. L-Cysteine and glutathione, due to their presence in biological systems, should be better model compounds than 2-mercaptoethanol.

In this study we characterize the kinetics of the thiolytic cleavage of *m*-AMSA and report for the first time that this reaction is acid catalyzed. Furthermore, the studies reported here together with the studies of the alkaline hydrolysis of 9-aminoacridine and few of its derivatives reported by Kalatzis<sup>3</sup> are the only systematic studies of the nucleophilic cleavage of acridine derivatives.

## Experimental Section

**Materials.** *m*-AMSA was obtained from NCI. L-Cysteine, glutathione, *N*-acetylcysteine, and 2-mercaptoethanol were obtained from Aldrich Chemical Co. and cysteamine was obtained from Sigma Chemical Co. All other chemicals used were also of reagent grade. Doubly glass-distilled water was used in the various studies.

**Kinetic Measurements.** The kinetic studies were carried out by monitoring the disappearance of *m*-AMSA at appropriate wavelengths by using a Beckman Model 3600 UV spectrophotometer. The wavelength 452 nm was used for monitoring the kinetics in buffer solutions of L-cysteine and cysteamine while 435 nm was selected for thiolysis in presence of all other thiol buffer solutions. The temperature of the reaction mixture was controlled at 30 °C electronically by using the temperature-control unit of spectrophotometer. All the kinetic runs were carried out at a constant ionic strength of 1.0 M except in case of L-cysteinolysis where it was kept constant at 2.0 M by using either potassium chloride or sodium sulfate salts. For a typical kinetic run, all the reaction ingredients except *m*-AMSA were placed in a 3-mL cuvette which was then put into the pretemperature-controlled cell compartment of the spectrophotometer for equilibration for about 10–15 min. The reaction was then started by adding 50  $\mu\text{L}$  of the concentrated stock solution of protonated form of *m*-AMSA prepared in methanol. This procedure added 2% methanol in all kinetic runs. All experiments were carried out in tightly stoppered glassware and cuvettes prepurged with nitrogen. The concentrations of all thiols were determined by weight. All the thiol buffer solutions were freshly prepared in degassed double-distilled water immediately before the start of

\* Author to whom inquiries should be addressed at Bayero University.

† Department of Pharmaceutics, College of Pharmacy, The Ohio State University, Columbus, OH.

(1) Denny, W. A.; Atwell, G. J.; Cain, B. F. *J. Med. Chem.* 1979, 22, 1453.

(2) Cain, B. F.; Wilson, W. R.; Baguley, B. C. *Mol. Pharmacol.* 1976, 12, 1027.

(3) Kalatzis, E. *J. Chem. Soc. B* 1969, 96.

Table I. Apparent Second- and Third-Order Rate Constants,  $k_n$  and  $k_{ga}$ , for Thiolysis of *m*-AMSA at 30 °C ( $\mu = 1.0$  M)

thiol	pH	$10^3 k_n, M^{-1} s^{-1}$	$10^3 k_{ga}, M^{-2} s^{-1}$	thiol	pH	$10^3 k_n, M^{-1} s^{-1}$	$10^3 k_{ga}, M^{-2} s^{-1}$
L-cysteine <sup>b</sup>	7.56	$0.352 \pm 0.081^a$	$6.450 \pm 0.301^a$	<i>N</i> -acetylcysteine	8.93	$0.728 \pm 0.095$	$12.46 \pm 0.45$
	8.02	$0.925 \pm 0.060$	$8.344 \pm 0.224$		9.22	$0.508 \pm 0.081$	$13.71 \pm 0.38$
	8.29	$0.730 \pm 0.051$	$10.020 \pm 0.202$		9.40	$0.473 \pm 0.032$	$12.92 \pm 0.15$
	8.40	$0.643 \pm 0.083$	$10.951 \pm 0.318$		9.65	$0.296 \pm 0.040$	$10.81 \pm 0.19$
	8.52	$0.738 \pm 0.075$	$10.578 \pm 0.298$		9.98	$0.275 \pm 0.097$	$5.91 \pm 0.46$
	8.72	$0.743 \pm 0.108$	$10.867 \pm 0.403$		11.40	$0.050 \pm 0.019^c$	
	9.28	$0.227 \pm 0.234$	$8.755 \pm 0.767$		2-mercaptoethanol	8.91	$0.418 \pm 0.054$
10.35	$0.078 \pm 0.068$	$1.910 \pm 0.231$	9.08	$0.402 \pm 0.033$		$9.256 \pm 0.131$	
glutathione	7.44	$4.636 \pm 0.166$	$34.66 \pm 1.14$	9.28		$0.339 \pm 0.026$	$8.667 \pm 0.101$
	7.56	$3.977 \pm 0.186$	$39.51 \pm 1.71$	9.47	$0.254 \pm 0.057$	$7.353 \pm 0.213$	
	7.85	$5.278 \pm 0.378$	$32.77 \pm 2.60$	9.88	$0.208 \pm 0.040$	$3.343 \pm 0.149$	
	8.29	$4.782 \pm 0.114$	$35.07 \pm 1.12$	cysteamine	7.78	$0.753 \pm 0.089$	$7.351 \pm 0.308$
	8.56	$4.873 \pm 0.155$	$35.29 \pm 1.52$		7.94	$0.882 \pm 0.052$	$7.666 \pm 0.193$
	8.74	$5.048 \pm 0.183$	$33.24 \pm 1.68$		8.05	$0.759 \pm 0.072$	$9.068 \pm 0.266$
	8.90	$4.131 \pm 0.364$	$34.55 \pm 2.62$		8.27	$0.761 \pm 0.049$	$10.03 \pm 0.18$
9.30	$3.073 \pm 0.138$	$22.88 \pm 1.21$	8.36		$0.636 \pm 0.060$	$10.43 \pm 0.24$	
9.75	$1.983 \pm 0.111$	$8.42 \pm 0.81$	8.46		$0.453 \pm 0.113$	$12.04 \pm 0.42$	
<i>N</i> -acetylcysteine	7.61	$1.940 \pm 0.323$	$9.980 \pm 1.530$		8.66	$0.674 \pm 0.098$	$10.04 \pm 0.36$
	8.41	$0.860 \pm 0.060$	$10.17 \pm 0.30$	8.87	$0.597 \pm 0.106$	$9.382 \pm 0.394$	
	8.55	$0.700 \pm 0.029$	$8.675 \pm 0.160$	9.08	$0.395 \pm 0.059$	$8.649 \pm 0.234$	

<sup>a</sup> Error limits are standard deviations. <sup>b</sup>  $\mu = 2.0$  M. <sup>c</sup> Obtained from  $k_{\text{obsd}} = k_o + k_n[\text{RS}]_T$ .

a kinetic run to avoid any significant probable oxidation. Four kinetic runs were performed simultaneously by using the multisample cell programmer unit of the spectrophotometer which minimized any further significant oxidation due to delaying other kinetic runs if only one kinetic run was carried out at a time at constant pH. The buffer solutions of desired pH of all thiols were prepared by adding an appropriate amount of sodium hydroxide solution. The pH measurements were carried out by using an Orion Research Digital Ionalyzer, Model 801A. The pH values of all kinetic reaction mixtures were obtained just before the start and at the end of the reaction, and a kinetic run was discarded if the difference between the pH values before the start and at the end of reaction was found to be  $\geq 0.02$  pH unit.

All the kinetic runs were carried out under pseudokinetic conditions where pseudo-first-order rate constants ( $k_{\text{obsd}}$ ) were evaluated from eq 1.

$$A_{\text{obsd}} = EX_0 \exp(-k_{\text{obsd}}t) + A_{\infty} \quad (1)$$

The nonlinear least-squares technique was used for the evaluation of three unknown parameters:  $k_{\text{obsd}}$ , the apparent molar absorption coefficient ( $E$ ), and the absorbance at infinite time ( $A_{\infty}$ ).  $X_0$  and  $A_{\text{obsd}}$  represent the initial concentration of *m*-AMSA and observed absorbance at any time ( $t$ ), respectively. A computer program (in BASIC) for the nonlinear least-squares technique has been developed, and the computations for all kinetic runs were carried out on a HP2000F computer. The data fittings were excellent in all kinetic runs. The percent deviations between  $A_{\text{obsd}}$  and  $A_{\text{calcd}}$  were less than 1% prior to 3–8 half-lives of the reactions.

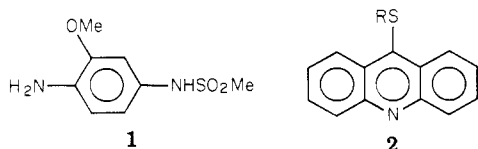
**Determination of  $pK_a$ .** The  $pK_a$  of *N*-acetylcysteine was determined potentiometrically at 30 °C and  $\mu = 1.0$  M by using eq 2, where  $\nu_R^-$  and  $\nu_{R^{2-}}$  are the activity coefficients corresponding

$$pK_a = \text{pH} + \log \left( \frac{[\text{HSRCO}_2^-] \nu_{R^-}}{[\text{SRCO}_2^{2-}] \nu_{R^{2-}}} \right) \quad (2)$$

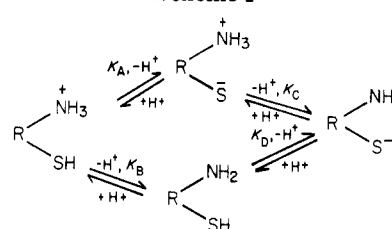
to mono- and dianionic forms of thiol. The activity coefficient  $\nu$  was calculated by using eq 3, where  $\mu$  is the ionic strength.

$$\log \nu = -0.52Z^2 \left( \frac{\mu^{1/2}}{(1 + \mu^{1/2})} - 0.2\mu \right) \quad (3)$$

**Product Characterization.** In a typical kinetic run containing glutathione buffer and *m*-AMSA, the TLC of reaction was carried out at different time intervals which revealed the formation of 4-amino-3-methoxy-methanesulfonanilide (1) as identified by using



Scheme I



an authentic sample of 1. Furthermore, the thioether 2 formed by the reaction of glutathione and *m*-AMSA has a characteristic strong absorption peak at  $\sim 363$  nm, where none of the other expected products has appreciable absorption. In a kinetic run containing glutathione buffer and *m*-AMSA, the spectra of reaction mixture scanned at different time intervals showed the appearance of a peak at  $\sim 363$  nm. The details of the study describing the initial as well as further product formation of the thiolysis of *m*-AMSA have been described elsewhere.<sup>4</sup>

## Results and Discussion

**(1) Reaction of L-Cysteine and Glutathione with *m*-AMSA.** A series of kinetic runs were carried out at various total buffer concentrations of amino thiols. The observed pseudo-first-order rate constants were found to follow eq 4, where  $[\text{ARS}]_T$  represents the total buffer

$$k_{\text{obsd}} = k_n[\text{ARS}]_T + k_{ga}[\text{ARS}]_T^2 \quad (4)$$

concentration and  $k_n$  and  $k_{ga}$  are rate constants for nucleophilic and general-acid-catalyzed thiolytic cleavage of *m*-AMSA. The rate constants  $k_n$  and  $k_{ga}$  were calculated by using the least-squares technique, and the results are summarized in Table I. The fit of  $k_{\text{obsd}}$  to eq 4 at several pH values is illustrated in Figure 1.

The equilibria of the various ionized species of an aminothiols<sup>5,6</sup> are illustrated in Scheme I. It is evident from earlier studies<sup>7</sup> on aminolysis of 9-aminoacridine and the one described in the present paper that the rate of aminolysis is much slower than the rate of thiolysis of acridine derivatives under essentially similar experimental conditions. This difference in reactivities of amines and thiols with acridines may be ascribed partly to the facts that amines and thiols are generally considered to be soft and

(4) Khan, M. N.; Malspeis, L., unpublished observations.

(5) Lindley, H. *Biochem. J.* 1962, 82, 418.

(6) Benesch, R. E.; Benesch, R. *J. Am. Chem. Soc.* 1955, 77, 5877.

(7) Wild, F.; Young, J. M. *J. Chem. Soc.* 1965, 7261.

hard nucleophiles,<sup>8</sup> respectively, and that since reactive centers in acridine derivatives are essentially soft electrophilic in nature, a soft nucleophile should be considered to be more reactive compared with a hard nucleophile with acridine derivatives. The spectral studies<sup>4</sup> of the product formation have also revealed the thiol groups of amino thiols acting as the nucleophiles in the degradation of *m*-AMSA studied in presence of amino thiol buffers. Thus, under the experimental conditions under which all the studies were carried out, it was believed that almost all ionized and unionized species of amino thiols were involved in thiolysis as either nucleophiles or general-acid catalysts. The general rate law of the thiolytic cleavage of *m*-AMSA may be given as in eq 5, where [*m*-AMSA]<sub>T</sub> represents the

$$-d[m\text{-AMSA}]_T/dt = k_0[m\text{-AMSA}]_T + (k_1[\text{H}_3\text{N}^+\text{RS}^-] + k_2[\text{H}_2\text{NRS}^-] + k_3[\text{H}_2\text{NRSH}] + k_4[\text{H}_3\text{N}^+\text{RSH}])[m\text{-AMSAH}^+] + (k_1'[\text{H}_3\text{N}^+\text{RS}^-] + k_2'[\text{H}_2\text{NRS}^-] + k_3'[\text{H}_2\text{NRSH}] + k_4'[\text{H}_3\text{N}^+\text{RSH}])[m\text{-AMSA}] + (k_5[\text{H}_3\text{N}^+\text{RSH}] + k_6[\text{H}_2\text{NRSH}])[ \text{H}_3\text{N}^+\text{RS}^- ] \times [m\text{-AMSA}^+\text{H}] + (k_5'[\text{H}_3\text{N}^+\text{RSH}] + k_6'[\text{H}_2\text{NRSH}])[ \text{H}_3\text{N}^+\text{RS}^- ] [m\text{-AMSA}] + (k_7[\text{H}_3\text{N}^+\text{RSH}] + k_8[\text{H}_2\text{NRSH}])[ \text{H}_2\text{NRS}^- ] [m\text{-AMSA}^+\text{H}] + (k_7'[\text{H}_3\text{N}^+\text{RSH}] + k_8'[\text{H}_2\text{NRSH}])[ \text{H}_2\text{NRS}^- ] [m\text{-AMSA}] + (k_9[m\text{-AMSA}^+\text{H}] + k_9'[m\text{-AMSA}])[ \text{H}_2\text{NRSH} ]^2 + (k_{10}[m\text{-AMSA}^+\text{H}] + k_{10}'[m\text{-AMSA}])[ \text{H}_3\text{N}^+\text{RSH} ]^2 \quad (5)$$

total concentration of *m*-AMSA,  $k_0$  is the rate constant for hydrolysis of *m*-AMSA, and [*m*-AMSA] and [*m*-AMSA<sup>+</sup>H] represent the concentrations of *m*-AMSA in the unprotonated and protonated forms, respectively.

The hydrolysis of *m*-AMSA, within a pH range of ~6–10, has appeared to be very slow compared with thiolysis. In order to get a reliable value of  $k_0$ , we carried out a few kinetic runs in phosphate and Tris buffer solutions for a period of more than 3 weeks. The observed rate constants were found to be on the order of  $10^{-7} \text{ s}^{-1}$  which is significantly smaller than even the standard deviations of the lowest obtained  $k_{\text{obsd}}$  values in thiolysis. Thus  $k_0$  is regarded as negligible in comparison to the thiolytic rate constants. Under such conditions, it can be shown that eq 6 and 7 follow from eq 5, where  $A = k_2K_CK_A + k_1'K_aK_A$

$$k_n = (A + Ba_H + k_4a_H^2 + k_2'K_CK_aK_Aa_H^{-1})(Qa_H/(a_H + K_a)) \quad (6)$$

$$k_{ga} = (C + Da_H + Ea_H^2 + Fa_H^3 + k_{10}a_H^4)(Q^2a_H/(a_H + K_a)) \quad (7)$$

$$+ k_3'K_BK_a, B = k_1K_A + k_3K_B + k_4'K_a, C = k_8'K_BK_CK_aK_A, D = k_6'K_BK_aK_A + k_9'K_B^2K_a + k_8K_BK_CK_a + k_7'K_CK_aK_A, E = k_6K_BK_a + k_9K_B^2 + k_5'K_aK_A + k_7K_CK_a, F = k_5K_A + k_{10}'K_a, \text{ and } Q = (a_H^2 + a_H(K_A + K_B) + K_AK_C)^{-1}.$$

(8) Hupe, D. J.; Jencks, W. P. *J. Am. Chem. Soc.* 1977, 99, 451.

(9) Figure 3 indicates that the observed point at pH 10.35 is nearly 10% deviated (positively) from linearity which could be attributed to the failure of the assumption that  $C$  is comparatively negligible at this pH. Thus a better value of  $D$  could be considered the observed point ( $4.13 \times 10^{-26} \text{ s}^{-1}$ ) at pH 9.28 which was found to be ~7% higher than the evaluated value of  $D$ . An attempt was made to fit the observed data to the following equation

$$k_{ga}(a_H + K_a)/a_HQ^2 = C + Da_H + Ea_H^2$$

within the pH range of 8.02–10.35. The least-squares-calculated values of  $C$ – $E$  were found to be  $(1.90 \pm 6.10) \times 10^{-26} \text{ M}^2 \text{ s}^{-1}$ ,  $(3.50 \pm 0.33) \times 10^{-26} \text{ M s}^{-1}$ , and  $(1.20 \pm 0.03) \times 10^{-17} \text{ s}^{-1}$ , respectively.

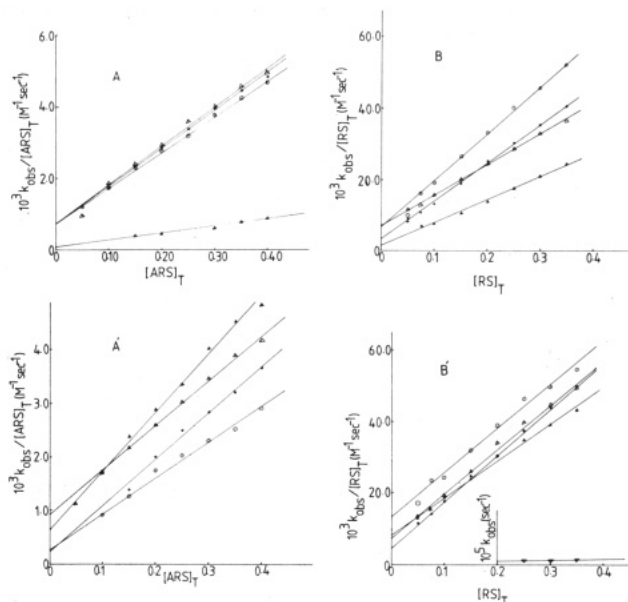


**Figure 1.** Observed second-order rate constants for thiolysis of *m*-AMSA as a function of the total concentration of thiol buffers at 30 °C. A and A': L-cysteine at pH values of (○) 8.29, (●) 8.52, (△) 8.72, and (▲) 10.35 and of (○) 7.56, (△) 8.02, (▲) 8.40, and (●) 9.28, respectively. B and B': N-acetylcysteine at pH values of (△) 8.55, (○) 9.22, (●) 9.65, and (▲) 9.98 and of (○) 7.61, (▲) 8.41, (△) 8.93, (●) 9.40, and (▽) 11.40, respectively. A plot of  $k_{\text{obsd}}$  ( $\text{s}^{-1}$ ) vs. total buffer concentration is inset.

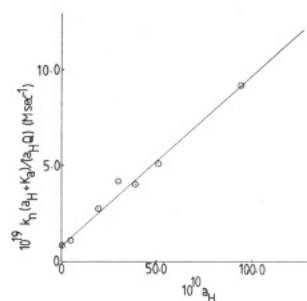


**Figure 2.** Plot of  $k_n(a_H + K_a)/a_HQ$  vs.  $a_H$  for the reaction of L-cysteine with *m*-AMSA. The solid line is drawn through the least-squares-calculated points by using eq 8 with  $A = 8.65 \times 10^{-20} \text{ M s}^{-1}$  and  $B = 8.71 \times 10^{-11} \text{ s}^{-1}$ .

The thiolytic cleavage of *m*-AMSA was studied in presence of L-cysteine buffer of varying pH ranging from 7.56 to 10.35. The plot of  $K_n(a_H + K_a)/Qa_H$  vs.  $a_H$  was found to be linear within the pH range of 8.02–10.35 (Figure 2). This linearity could be explained by assuming that  $(A + Ba_H) \gg (k_4a_H^2 + k_2'K_CK_aK_Aa_H^{-1})$ . Considering the numerical values of various microscopic ionization constants of amino thiols, one can expect the significant contribution of  $k_4a_H^2$  term compared with others only at pHs much below the  $\text{p}K_A$  as well as the  $\text{p}K_a$ , and, similarly, the significant contribution of  $k_2'K_CK_aK_A/a_H$  can be expected only at a pH much higher than the  $\text{p}K_C$ . Thus, within the observed pH range of 8.02–10.35, in case of L-cysteinolysis of *m*-AMSA, eq 6 becomes eq 8.

$$k_n(a_H + K_a)/(a_HQ) = A + Ba_H \quad (8)$$

A linear least-squares treatment was applied to obtain  $A = (8.65 \pm 1.21) \times 10^{-20} \text{ M s}^{-1}$  and  $B = (8.71 \pm 0.38) \times 10^{-11} \text{ s}^{-1}$ . The values of  $k_2$  and  $k_1'$  could be calculated from  $A$  as described in the Appendix (part I) and are summarized in Table II. The value of  $k_1$  was calculated as follows:  $B = k_1K_A + k_3K_B + k_4'K_a$ , within the pH range of 8.02–10.35,  $k_1K_A \gg (k_3K_B + k_4'K_a)$ , and hence  $k_1 = B/K_A$ , whereby

Table II.<sup>a</sup> Nucleophilic Second-Order Rate Constants,  $k_n$ , and General-Acid-Catalyzed Rate Constants,  $k_{ga}$ , for Thiolytic Cleavage of *m*-AMSA (Free Base) and 4 at 30 °C

RSH	$pK_a$	$k_n, M^{-1} s^{-1}$	$pK_a$	$k_{ga}, M^{-2} s^{-1}$
HSCH <sub>2</sub> CH(NH <sub>2</sub> )CO <sub>2</sub> <sup>-</sup>	9.56 <sup>b</sup>	$10^2 k_2 = 5.61 \pm 0.80^c$	9.56	$10^2 k_6' = 1.96 \pm 0.10^c$
HSCH <sub>2</sub> CH(NH <sub>3</sub> <sup>+</sup> )CO <sub>2</sub> <sup>-</sup>	8.21 <sup>b</sup>	$10^2 k_1 = 1.41 \pm 0.06$	8.21	$10^2 k_7' = 9.26 \pm 0.47$
	8.21	$10^4 k_1' = 1.81 \pm 0.08$	8.21	$10^2 k_5' = 4.08 \pm 0.14$
	8.72 <sup>b</sup>	$10 k_1 = 1.60 \pm 0.04$	8.72	$10^2 k_5' = 6.78 \pm 0.46$
	8.72	$10^4 k_1' = 3.18 \pm 0.64$	8.72	$k_5 = 1.13 \pm 0.01$
	8.72	$10^4 k_1'e = 4.03 \pm 0.18$	8.72	$10^2 k_{10} = 3.0 \pm 06$
			8.72	$10 k_6' = 2.32 \pm 0.12$
	9.47 <sup>b</sup>	$10 k_2 = 6.57 \pm 1.32$		
	9.47 <sup>b</sup>	$10 k_2^e = 8.32 \pm 0.38$		
	9.95 <sup>d</sup>	$10^5 k_1' = 5.16 \pm 2.00$	9.95	$10^3 k_3' = 3.52 \pm 1.35$
	9.95	$10^3 k_2 = 4.55 \pm 0.17$	9.95	$10^3 k_5' = 9.54 \pm 1.44$
	9.95	$10 k_1 = 2.45 \pm 0.19$	9.95	$k_3 = 1.24 \pm 0.19$
			9.95	$10^2 k_5 = 1.06$
			10.0 <sup>b</sup>	$k_4 = 2.04 \pm 0.90$
HSCH <sub>2</sub> CH <sub>2</sub> OH	9.45 <sup>b</sup>	$10^5 k_1' = 4.75 \pm 4.26$	9.45	$10^2 k_3' = 1.11 \pm 0.26$
	9.45	$10^2 k_1 = 7.02 \pm 0.28$	9.45	$10^3 k_5' = 9.45 \pm 0.15$
			9.45	$k_3 = 1.08 \pm 0.17$
SCH <sub>2</sub> CH <sub>2</sub> OH			>16	$k_4 = 1.49 \pm 0.19$
HSCH <sub>2</sub> CH <sub>2</sub> NH <sub>3</sub> <sup>+</sup>	8.22 <sup>b</sup>	$10^4 k_1' = 3.31 \pm 1.10$	8.22	$10^3 k_4' = 5.86 \pm 1.01$
	8.22	$10^2 k_1 = 1.01 \pm 0.06$	8.22	$10^2 k_3' = 4.02 \pm 0.10$

<sup>a</sup> The various rate constants summarized in this table represent the same constants defined in eq 5. <sup>b</sup> Reuben and Bruce.<sup>18</sup> <sup>c</sup> Error limits are standard deviations. <sup>d</sup> This study. <sup>e</sup> Calculated from  $5.72 \times 10^{-19} M s^{-1}$  (the observed point at pH 9.30) as described in the text.

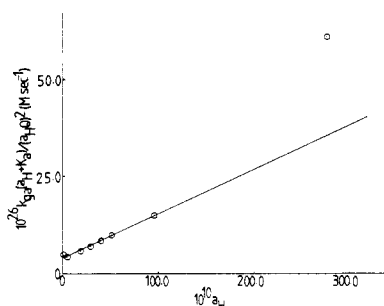


Figure 3. Plot of  $k_{ga}(a_H + K_a)/(a_H Q)^2$  vs.  $a_H$  for the reaction of L-cysteine with *m*-AMSA. The solid line is drawn through the least-squares-calculated points by using eq 9 with  $D = 3.85 \times 10^{-26} M s^{-1}$  and  $E = 1.15 \times 10^{-17} s^{-1}$ .

on substitution of the observed  $K_A$ ,  $k_1$  was calculated and is shown in Table II.

Figure 3 shows the plot of  $k_{ga}(a_H + K_a)/(Qa_H)^2$  vs.  $a_H$  which is linear within the pH range of 8.02–10.35. This indicates that under such conditions,  $Da_H + Ea_H^2$  should be much larger than  $C + Fa_H^3 + k_{10}a_H^4$ . Taking consideration of various microscopic ionization constants, one should expect the term  $C$  to be significant at a pH significantly higher than  $pK_C^9$ , and, similarly,  $Fa_H^3$  and  $k_{10}a_H^4$  should be significant at a pH less than or equal to  $pK_A$ . Thus eq 7 becomes eq 9. The constants  $D$  and  $E$ , calcu-

$$k_{ga}(a_H + K_a)/(Qa_H)^2 = D + Ea_H \quad (9)$$

lated by the least-squares technique, were found to be  $(3.85 \pm 0.19) \times 10^{-26} M s^{-1}$  and  $(1.15 \pm 0.04) \times 10^{-17} s^{-1}$ , respectively. The various microscopic rate constants were calculated from  $D$  and  $E$  as described in the Appendix (part II) and are summarized in Table II.

Figure 3 also indicates that the observed point at pH 7.56 is nearly 70% off (positively) from linearity. This shows that at pH 7.56, the contribution due to the  $Fa_H^3$  term to the rate compared with other terms is possibly no longer negligible.

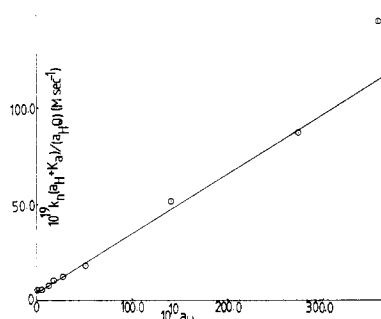
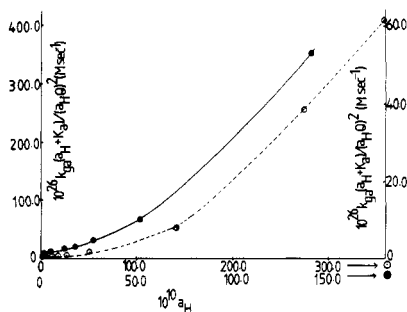
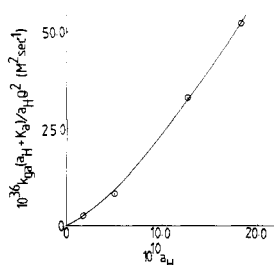


Figure 4. Plot of  $k_n(a_H + K_a)/a_H Q$  vs.  $a_H$  for the reaction of glutathione with *m*-AMSA. The solid line is drawn through the least-squares-calculated points by using eq 8 with  $A = 4.52 \times 10^{-19} M s^{-1}$  and  $B = 3.05 \times 10^{-10} s^{-1}$ .

The thiolytic cleavage of *m*-AMSA with glutathione buffer was studied at various pHs ranging from 7.44 to 9.75 at 30 °C. The graphical representation of the variation of  $k_n$  with  $a_H$  is shown in Figure 4 as a plot of  $k_n(a_H + K_a)/a_H Q$  vs.  $a_H$ . The plot was found to be linear within the pH range of 7.56–9.75, and hence to explain this linear relationship, we assume that  $(A + Ba_H) \gg (k_4 a_H^2 + k_2' K_C K_A K_A a_H^{-1})$ . This assumption could be justified by considering the microscopic ionization constants of glutathione to be equal to  $k_4 a_H^2$  and to be significant in comparison to other terms only at pHs where  $[m\text{-AMSA}]$  and the concentrations of ionized thiol would be much smaller than  $[m\text{-AMSA}^+H]$  and  $[H_3N^+RSH]$ . At pH 7.56,  $[m\text{-AMSA}]$  would be 58% of the total concentration of substrate, and hence a comparatively significant contribution of  $k_4 a_H^2$  would be unlikely. Similarly, the  $k_2'$  term would be expected at pHs greater than  $pK_C$  (9.47). Only one value of  $k_n$  was observed at pH 9.75, but the point was not found to be deviated appreciably from linearity (Figure 4). Thus, under the observed pH range, eq 6 becomes eq 8. A linear least-squares technique was used to evaluate the values of  $A$  and  $B$  which were found to be  $(4.52 \pm 0.91) \times 10^{-19} M s^{-1}$  and  $(3.05 \pm 0.08) \times 10^{-10} s^{-1}$ , respectively.



**Figure 5.** Plot of  $k_{ga}(a_H + K_a)/(a_H Q)^2$  vs.  $a_H$  with both a left-hand-side (O) and a right-hand-side ordinate (●) for the reaction of glutathione with *m*-AMSA. The solid line is drawn through the least-squares-calculated points by using eq 11 with  $D = 1.37 \times 10^{-26} \text{ M s}^{-1}$ ,  $E = 0.059 \times 10^{-16} \text{ s}^{-1}$ , and  $F = 2.16 \times 10^{-9} \text{ M}^{-1} \text{ s}^{-1}$ .



**Figure 6.** Plot of  $k_{ga}(a_H + K_a)/(a_H Q)^2$  vs.  $a_H$  for the reaction of glutathione with *m*-AMSA. The solid line is drawn through the least-squares-calculated points by using eq 10 with  $C = -0.77 \times 10^{-36} \text{ M}^2 \text{ s}^{-1}$ ,  $D = 1.55 \times 10^{-26} \text{ M s}^{-1}$ , and  $E = 0.087 \times 10^{-16} \text{ s}^{-1}$ .

The obtained value of  $A$  was used to calculate  $k_2$  and  $k_1'$  as described in the Appendix (part I). The calculated values of  $k_2^{10}$  and  $k_1'$  are shown in Table II. Similarly, the observed value of  $B$  was used to calculate the value of  $k_1$  ( $=B/K_A$ , provided  $k_1 K_A \gg (k_3 K_B + k_4' K_a)$  which is shown in Table II.

The plot of  $k_{ga}(a_H + K_a)/Q^2 a_H^2$  vs.  $a_H$  is shown in Figure 5. This plot revealed that apparently there was not any region within the observed pH range where the pH-rate profile appeared to be linear. In order to get a reliable value of constant  $C$ , we fitted the observed data at various pHs varying from 8.74 to 9.75 to eq 10. This pH range

$$k_{ga}(a_H + K_a)/Q^2 a_H^2 = C + D a_H + E a_H^2 \quad (10)$$

was believed to be the one under which the contribution of the  $C$  term would be significant. The constants  $C$ – $E$  as evaluated by the least-squares technique were found to be  $(-0.77 \pm 1.01) \times 10^{-36} \text{ M}^2 \text{ s}^{-1}$ ,  $(1.55 \pm 0.27) \times 10^{-26} \text{ M s}^{-1}$ , and  $(0.087 \pm 0.013) \times 10^{-16} \text{ s}^{-1}$ , respectively. The fitting of the data is evident from the plot (Figure 6) where solid line is drawn through the calculated points. The negative value of  $C$  with a standard deviation of more than 100% is statistically not different from zero. Thus, on the assumption that  $C$  is negligible compared with other terms, the observed data were fitted to eq 11.

$$k_{ga}(a_H + K_a)/Q^2 a_H^2 = D + E a_H + F a_H^2 \quad (11)$$

A linear least-squares treatment resulted in values of  $D$ – $F$  of  $(1.37 \pm 0.07) \times 10^{-26} \text{ M s}^{-1}$ ,  $(0.059 \pm 0.004) \times 10^{-16} \text{ s}^{-1}$ , and  $(2.16 \pm 0.02) \times 10^{-9} \text{ M}^{-1} \text{ s}^{-1}$ , respectively. From

(10) As  $a_H \rightarrow 0$ , the  $k_2'$  term should be effective; as a result, at pHs higher than  $\sim 9.40$  the observed point should be expected to deviate positively ( $\text{Lim } a_H \rightarrow 0, k_2' K_C K_A K_a / a_H \rightarrow \infty$ ), and the  $\sim 8\%$  deviation of the observed point at pH 9.75 (Figure 4) is possibly an indication of the relative significance of the  $k_2'$  term. Thus the better value of  $A$  to calculate  $k_2$  would be the observed point at pH 9.30. The value of  $k_2$  was thus calculated by using the observed point ( $5.72 \times 10^{-19} \text{ M}^{-1} \text{ s}^{-1}$ ) and is shown in Table II.

the fairly good fitting of the observed data to eq 11 (Figure 5) it was concluded that the contribution of the  $k_{10}$  term was negligible within the pH range 7.85–9.75. Since the  $pK_a$  of *m*-AMSA is 7.34, a comparative significant contribution of the  $k_{10}$  term can be expected at pH  $\sim 7.34$ . Figure 5 revealed that the observed points at pH 7.56 and 7.44 were 41% and 37% off positively, which in turn showed that at these pHs the contribution due to  $k_{10}$  was no longer negligible. The value of  $k_{10}$  was calculated by substituting the values of  $C$ – $F$  in eq 7, and thus the average value was found to be  $0.030 \pm 0.006 \text{ M}^{-2} \text{ s}^{-1}$ . The various general-acid-catalyzed rate constants could be calculated from observed values of  $D$ – $F$  as in eq 12 because under the

$$D = k_6' K_B K_a K_A + k_9' K_B^2 K_a + k_8 K_B K_C K_a + k_7' K_C K_a K_A = (k_6' + k_7') K_B K_a K_A \quad (12)$$

experimental conditions ( $k_6' K_B K_a K_A + k_7' K_C K_a K_A \gg (k_9' K_B^2 K_a + k_8 K_B K_C K_a)$ ) and  $K_B = K_C$ . In eq 12,  $k_6' = k_7'$  because  $K_B = K_C$  and  $K_A = K_D$ , and the value of  $k_6'$  calculated from eq 12 is shown in Table II. The value of  $k_5'$  was calculated as described in the Appendix (part II) and is shown in Table II. Similarly,  $F = k_5' K_a$  provided  $k_5' K_A > k_{10}' K_a$ . The value of  $k_5'$  thus calculated is also given in Table II.

(2) **Reaction of *N*-Acetylcysteine, 2-Mercaptoethanol, and Cysteamine.** To determine the nucleophilic as well as the buffer catalysis of these thiols, we carried out the kinetic runs at different buffer concentrations and at constant pH and ionic strength. The observed pseudo first-order rate constants,  $k_{\text{obsd}}$ , were found to be well-fitted to eq 13, where  $[\text{RS}]_T$  represents the total concentration

$$k_{\text{obsd}} = k_n [\text{RS}]_T + k_{ga} [\text{RS}]_T^2 \quad (13)$$

of buffer of monofunctional thiol.  $k_n$  and  $k_{ga}$  are nucleophilic and general-acid-catalyzed rate constants for thiolysis. The rate constants  $k_n$  and  $k_{ga}$  were evaluated from eq 13 by using the linear least-squares technique. The thiolysis of *m*-AMSA was studied at various pHs of the reaction medium, and the respective values of  $k_n$  and  $k_{ga}$  are summarized in Table I. The observed data are shown graphically in Figure 1. In these figures the solid lines are drawn through the calculated values of rate constants which in turn give the degree of fitting of observed data to eq 13.

Despite the existence of an amino group in cysteamine, it has no microscopic ionization constants as shown in Scheme I for L-cysteine and glutathione.<sup>6</sup> (One of the referees of the *Journal of the American Chemical Society* has suggested that cysteamine does have microscopic ionization constants, however, and that  $K_A \approx 20K_B$ . Unfortunately, he did not mention the reference as well as the absolute values of  $K_A$ ,  $K_B$ ,  $K_C$ , and  $K_D$ .) As has been discussed before, it is the thiol group of cysteamine which is the reacting group in the degradation of *m*-AMSA. Thus for a thiol of the type RSH, the rate of thiolytic cleavage of *m*-AMSA may be given as eq 14.

$$-d[m\text{-AMSA}]_T/dt = (k_1 [\text{RS}^-] + k_2 [\text{RSH}]) \times [m\text{-AMSAH}^+] + (k_1' [\text{RS}^-] + k_2' [\text{RSH}]) [m\text{-AMSA}] + (k_3 [\text{RS}^-] [\text{RSH}] + k_4 [\text{RS}^-]^2 + k_5 [\text{RSH}]^2) [m\text{-AMSAH}^+] + (k_3' [\text{RS}^-] [\text{RSH}] + k_4' [\text{RS}^-]^2 + k_5' [\text{RSH}]^2) [m\text{-AMSA}] \quad (14)$$

Equation 14 can be used to derive eq 15 and 16.

$$k_n = \frac{k_1' K K_a + (k_1 K + k_2' K_a) a_H + k_2 a_H^2}{(a_H + k_a)(a_H + K)} \quad (15)$$

$$k_{ga} = [k_4' K^2 K_a + (k_4 K^2 + k_3' K_a K) a_H + (k_3 K + k_5' K_a) a_H^2 + k_5 a_H^3] / (a_H + K_a)(a_H + K)^2 \quad (16)$$

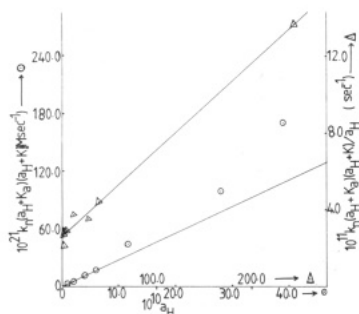


**Figure 7.** Plots showing the dependence of (O)  $k_n(a_H + K)(a_H + K_a)$  and ( $\Delta$ )  $k_n(a_H + K)(a_H + K_a)/a_H$  vs.  $a_H$  for the reaction of *N*-acetylcysteine with *m*-AMSA. The solid lines are drawn through the least-squares-calculated points by using eq 19 for  $k_1'KK_a = -1.02 \times 10^{-21} \text{ M s}^{-1}$  and  $k_1K + k_2'K_a = 2.96 \times 10^{-11} \text{ s}^{-1}$  (O) and eq 15 for  $k_1K + k_2'K_a = 2.53 \times 10^{-11} \text{ s}^{-1}$  and  $k_2 = 4.55 \times 10^{-3} \text{ M}^{-1} \text{ s}^{-1}$  ( $\Delta$ ).

A plot of  $k_n(a_H + K_a)(a_H + K)$  vs.  $a_H$  for *N*-acetylcysteinolysis of *m*-AMSA is shown in Figure 7 which indicates that within the pH range of 9.98–9.22, the plot is essentially linear with an intercept not statistically different from zero. The observed thermodynamic  $pK_a$  of *N*-acetylcysteine is 9.95 at 30 °C, and hence at pH 9.98 one would expect only about 50% of the total amount of thiol to exist in ionized form. Thus at pH values lower than 9.98, the contribution due to the  $k_1'$  step may be considered to be negligible compared with that of the  $k_2'$  step of the kinetically equivalent  $k_1$  step. A few kinetic runs were carried out at pH 11.40 where nearly 97% of the thiol would exist in an ionized form, and the observed pseudo-first-order rate constants were found to follow eq 17 as

$$k_{\text{obsd}} = k_0 + k_n[\text{RS}]_T \quad (17)$$

shown graphically in Figure 1. Equation 17 indicates that at pHs where the amount of unionized form of thiol is  $\leq 3\%$ , the general-acid-catalyzed term is no longer sensitive to the rate law. However, under such conditions the rate constant  $k_n$  can be used to estimate the upper limit for the value of  $k_1'$ . A linear least-squares treatment gave  $10^5 k_0 = 2.54 \pm 0.59 \text{ s}^{-1}$  and  $10^5 k_n = 5.00 \pm 1.94 \text{ M}^{-1} \text{ s}^{-1}$ . At pH 11.40, eq 15 reduces to eq 18, from which the calculated value of  $k_1'$  is  $5.16 \times 10^{-5} \text{ M}^{-1} \text{ s}^{-1}$ .

$$k_n = k_1'KK_a/(a_H + K_a)(a_H + K) \quad (18)$$

The linearity of the plot (Figure 7) within the pH range 9.98–9.22 indicated that the  $k_2$  term was negligible compared with the other terms of eq 15.

Thus, under such conditions eq 15 reduced to eq 19. A

$$k_n = \frac{k_1'KK_a + (k_1K + k_2'K_a)a_H}{(a_H + K)(a_H + K_a)} \quad (19)$$

linear least-squares treatment was used to calculate  $k_1'KK_a$  and  $k_1K + k_2'K_a$ , and they were found to be  $(-1.02 \pm 0.92) \times 10^{-21} \text{ M s}^{-1}$  and  $(2.96 \pm 0.24) \times 10^{-11} \text{ s}^{-1}$ , respectively.

Below pH 9.22, the experimental points started deviating from the linear plot (Figure 7) which indicated that the assumption  $k_2a_H^2 \ll (k_1K + k_2'K_a)a_H$  was no longer true. Under such conditions, a plot of  $k_n(a_H + K_a)(a_H + K)/a_H$  vs.  $a_H$  was found to be linear (Figure 7), and the intercept  $(k_1K + k_2'K_a)$  and slope ( $k_2$ ) of this plot were found to be  $(2.53 \pm 0.16) \times 10^{-11} \text{ s}^{-1}$  and  $(4.55 \pm 0.17) \times 10^{-3} \text{ M}^{-1} \text{ s}^{-1}$ . The average value  $((2.75 \pm 0.21) \times 10^{-11} \text{ s}^{-1})$  of  $k_1K + k_2'K_a$  was used to calculate  $k_1$  by assuming  $k_2'K_a < k_1K$ , and the value thus obtained is shown in Table II. The condition that  $k_2'K_a > k_1K$  could be ruled out on the basis of the calculated value of  $k_2'$  ( $6.0 \times 10^{-4} \text{ M}^{-1} \text{ s}^{-1}$ ) obtained by use of this condition. This value of  $k_2'$  is nearly 15 times larger than  $k_1'$  which is unlikely.

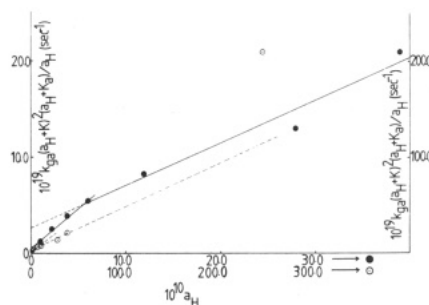


**Figure 8.** Plot of  $k_{ga}(a_H + K)^2(a_H + K_a)/a_H$  vs.  $a_H$  with both a left-hand-side ordinate ( $\bullet$ ) and a right-hand-side ordinate ( $\circ$ ) for the reaction of *N*-acetylcysteine with *m*-AMSA. The solid lines are drawn through the least-squares-calculated points by using eq 21 with  $C_1 = 5.08 \times 10^{-20} \text{ s}^{-1}$  and  $m_1 = 8.27 \times 10^{-10} \text{ M}^{-1} \text{ s}^{-1}$  (within the pH range of 9.98–9.22) and eq 22 with  $C_2 = 2.55 \times 10^{-19} \text{ s}^{-1}$  and  $m_2 = 4.36 \times 10^{-10} \text{ M}^{-1} \text{ s}^{-1}$  (within the pH range of 9.22–8.41).

The plot of  $k_{ga}(a_H + K_a)(a_H + K)^2/a_H$  vs.  $a_H$  as shown in Figure 8 indicated a change in slope with a change of pH. Within the pH range 9.98–9.22 the plot was linear with an intercept of  $C_1 = (5.08 \pm 1.95) \times 10^{-20} \text{ s}^{-1}$  and a slope of  $m_1 = (8.27 \pm 0.51) \times 10^{-10} \text{ M}^{-1} \text{ s}^{-1}$ , and then the intercept ( $C_2$ ) and slope ( $m_2$ ) changed to  $(2.55 \pm 1.65) \times 10^{-19} \text{ s}^{-1}$  and  $(4.36 \pm 0.66) \times 10^{-10} \text{ M}^{-1} \text{ s}^{-1}$ , respectively, within the pH range 9.22–8.41. These observations revealed that the  $k_4'K_aK^2$  and  $k_5a_H^3$  terms were negligible in comparison to the other terms in eq 16. On consideration of the  $pK_a$  of the thiol and substrate, this assumption appeared to be likely, for  $k_4'K_aK^2$  could be expected to be comparatively significant only at a pH much higher than the  $pK_a$ s of the thiol and substrate, and the ionized thiol provided should have an acidic group to act as a general acid in catalysis. Likewise,  $k_5a_H^3$  term could be expected at lower pH than the  $pK_a$ s of thiol and substrate. Thus, within the pH range 9.98–8.41 eq 16 reduces to eq 20.

$$K_{ga}(a_H + K_a)(a_H + K)^2/a_H = \frac{k_4K^2 + k_3'KK_a + (k_3K + k_5'K_a)a_H}{(20)}$$

The break in the pH rate profile (Figure 8) could be explained by assuming that, within the pH range 9.98–9.22,  $k_4K^2 \ll k_3'K_aK$ , probably because of the extremely low concentration of *m*-AMSA<sup>+</sup>H and not a sufficiently high concentration of RS<sup>-</sup>. Thus, the application of this assumption reduced eq 20 to eq 21. The calculated value

$$k_{ga}(a_H + K_a)(a_H + K)^2/a_H = k_3'KK_a + (k_3K + k_5'K_a)a_H \quad (21)$$

of  $k_3'$  ( $=C_1/K_aK$ ) is shown in Table II. The decrease in the value of  $m_2$  compared with  $m_1$  within the pH range 9.22–8.55 could be explained by assuming that  $k_3K \ll k_5'K_a$ . This assumption seemed to be likely because at pH values lower than 9.22, the concentrations of ionized thiol and protonated *m*-AMSA would not be sufficient to make the  $k_3$  term significant compared with  $k_5'K_a$ . Furthermore, the increase in  $C_2$  compared with  $C_1$  revealed that the assumption  $k_4K^2 \ll k_3'K_aK$  was no longer true.<sup>11</sup> With

(11) The  $k_4$  term, in the *N*-acetylcysteinolysis of *m*-AMSA, seems to be fortuitous, for it is unlikely for an ionized thiol to act as a general-acid catalyst. A remote possibility of a species acting as general-acid catalyst is the hydrolyzed product  $H_3N^+RS^-$  of *N*-acetylcysteine. The hydrolysis of *N*-acetylcysteine should be much slower than thiolysis within the observed pH range. However, an intramolecular general-base-catalyzed hydrolysis should be much faster than the one having no such intramolecularly facilitating group. Such types of enhanced reactivity have been observed in many reactions.<sup>12</sup> But since the  $pK_C (=10)$  of L-cysteine is almost similar to the  $pK_a$  of *N*-acetylcysteine, the chances of errors in the calculated values of other rate constants will be negligible.

these assumptions, eq 20 changed to eq 22. The calculated

$$k_{ga}(a_H + K_a)(a_H + K)^2 = k_4K^2 + k_3'K_aK + k_5'K_a a_H \quad (22)$$

value of  $k_5'$  ( $=m_2/K_a$ ) is shown in Table II. The values of  $k_3$  and  $k_4$ , as shown in Table II, were calculated from the respective values of  $m_1$  and  $C_2$  by substitution of the calculated values  $k_5'$  and  $k_3'$ , respectively, in eq 22.

The decrease in pH from 8.41 caused a positive deviation in the observed point from linearity as is evident from Figure 8. The observed point at pH 7.61 is ~58% larger than the one expected from linearity. This showed that under these experimental conditions the  $k_5a_H^3$  term was no longer negligible in comparison to the other terms of the rate law. The observed point at pH 7.61 was used for calculation of  $k_5$  by substituting the value of  $C_2$  and  $m_2$  in eq 16, and the value thus obtained is  $0.0106 \text{ M}^{-2} \text{ s}^{-1}$ .

The thiolysis of *m*-AMSA involving 2-mercaptoethanol was studied within the pH range 8.91–9.88. The plot of  $k_n(a_H + K_a)(a_H + K)$  vs.  $a_H$ , as shown in Figure 9, is linear, and hence under these conditions,  $k_2a_H^2 \ll (k_1KK_a + (k_1K + k_2'K_a)a_H)$ . Thus eq 15 becomes eq 19. The least-squares-calculated values of  $k_1'KK_a$  and  $k_1K + k_2'K_a$  were found to be  $(7.70 \pm 6.91) \times 10^{-22} \text{ M s}^{-1}$  and  $(2.49 \pm 0.10) \times 10^{-11} \text{ s}^{-1}$ , respectively. The calculated values of  $k_1'$  obtained from the intercept and of  $k_1$  obtained from slope (provided that  $k_1K \gg k_2'K_a$ ) are summarized in Table II.

A plot of  $k_{ga}(a_H + K)^2(a_H + K_a)$  vs.  $a_H$  was found to be nonlinear. But, however, a plot of  $k_{ga}(a_H + K)^2(a_H + K_a)/a_H$  vs.  $a_H$  as shown in Figure 10 appeared to be linear within the pH ranges (i) 9.88–9.28 with intercept ( $C_1$ ) and slope ( $m_1$ ) equal to  $(1.80 \pm 0.43) \times 10^{-19} \text{ s}^{-1}$  and  $(8.15 \pm 1.19) \times 10^{-10} \text{ M}^{-1} \text{ s}^{-1}$ , respectively, and (ii) 9.28–8.91 with intercept ( $C_2$ ) and slope ( $m_2$ ) equal to  $(3.67 \pm 0.06) \times 10^{-19} \text{ s}^{-1}$  and  $(4.32 \pm 0.07) \times 10^{-10} \text{ M}^{-1} \text{ s}^{-1}$ , respectively. As has been discussed before in the *N*-acetylcysteinolysis of *m*-AMSA, the observed data, within the pH ranges 9.88–9.28 and 9.28–8.91, were considered to follow eq 21 and 22, respectively, and the calculated values of  $k_4$ ,  $k_3'$ ,  $k_3$ , and  $k_5'$  are summarized in Table II. The observed data also revealed that  $k_4'K^2K_a$  and  $k_5a_H^3$  were negligible compared with the other terms of eq 16.

The thiolysis of *m*-AMSA was also studied by using buffer solutions of cysteamine at varying pH, ranging from 7.78 to 9.08. Figure 11 shows the plot of  $k_n(a_H + K_a)$  vs.  $a_H$ . The plot is nearly linear over the entire pH range studied. This observation indicates that under such conditions, i.e.,  $k_2a_H^2 \ll (k_1KK_a + (k_1K + k_2'K_a)a_H)$ , which seems to be likely because even at the lowest observed pH (7.78), nearly 26% of the total cysteamine will exist in the ionized form. This makes the  $k_2$  terms negligible compared with  $k_1$  and  $k_1'$ . Thus, in this case, eq 19 was found to be followed by the observed data. The intercept ( $k_1'KK_a$ ) and slope ( $k_1K + k_2'K_a$ ) were found to be  $(9.11 \pm 3.02) \times 10^{-20} \text{ M s}^{-1}$  and  $(6.11 \pm 0.38) \times 10^{-11} \text{ s}^{-1}$ , respectively. The calculated value of  $k_1'$  from the intercept with known values of  $K$  and  $K_a$  and that of  $k_1$  from slope, assuming  $k_1K \gg k_2'K_a$ , are summarized in Table II.

The plot of  $k_{ga}(a_H + K)^2(a_H + K_a)$  vs.  $a_H$  was found to be linear (Figure 12) within the pH range 7.94–9.08. To justify this linearity we assumed that  $k_4'K^2K_a + (k_4K^2 + k_3'K_aK)a_H \gg (k_3K + k_5'K_a)a_H^2 + k_5a_H^3$ . This assumption seemed to be satisfying on the grounds that amino group of the ionized cysteamine which would exist in the protonated form would be acting as a general acid even at the

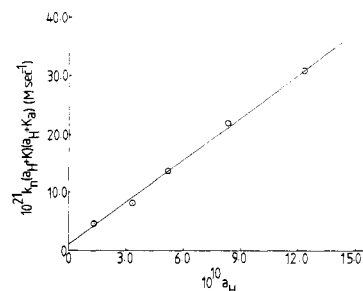


Figure 9. Plot of  $k_n(a_H + K)(a_H + K_a)$  vs.  $a_H$  for the reaction of 2-mercaptoethanol with *m*-AMSA. The solid line is drawn through the least-squares-calculated points by using eq 19 with  $k_1'KK_a = 7.70 \times 10^{-22} \text{ M s}^{-1}$  and  $k_1K + k_2'K_a = 2.49 \times 10^{-11} \text{ s}^{-1}$ .

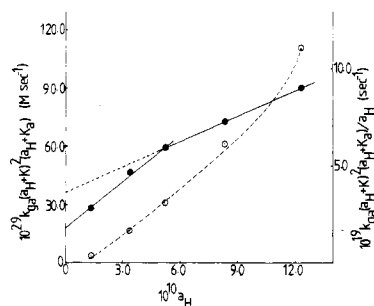


Figure 10. Plots showing the dependence of  $k_{ga}(a_H + K)^2(a_H + K_a)$  vs.  $a_H$  with a left-hand-side ordinate (O) and of  $k_{ga}(a_H + K)^2(a_H + K_a)/a_H$  vs.  $a_H$  with a right-hand-side ordinate (●) for the reaction of 2-mercaptoethanol with *m*-AMSA. The solid lines are drawn through the least-squares-calculated points by using eq 21 with  $C_1 = 1.80 \times 10^{-19} \text{ s}^{-1}$  and  $m_1 = 8.15 \times 10^{-10} \text{ M}^{-1} \text{ s}^{-1}$  (within the pH range of 9.88–9.28) and eq 22 with  $C_2 = 3.67 \times 10^{-19} \text{ s}^{-1}$  and  $m_2 = 4.32 \times 10^{-10} \text{ M}^{-1} \text{ s}^{-1}$  (within the pH range of 9.28–8.91).

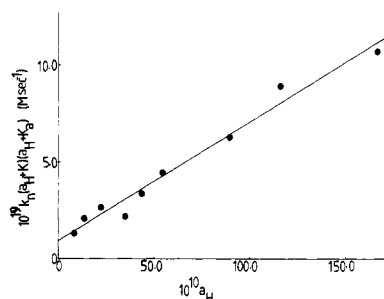


Figure 11. Plot of  $k_n(a_H + K)(a_H + K_a)$  vs.  $a_H$  for the reaction of cysteamine with *m*-AMSA. The solid line is drawn through the least-squares-calculated points by using eq 19 with  $k_1'KK_a = 9.11 \times 10^{-20} \text{ M s}^{-1}$  and  $k_1K + k_2'K_a = 6.11 \times 10^{-11} \text{ s}^{-1}$ .

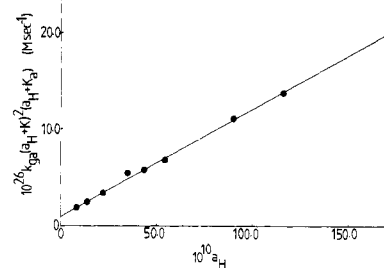
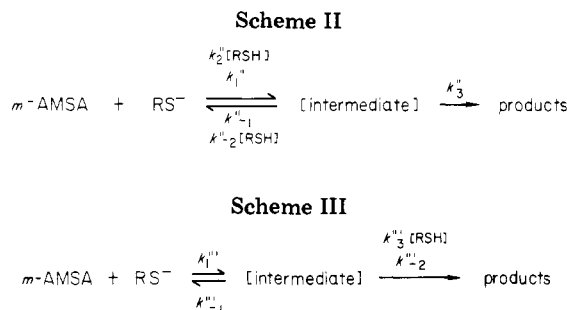


Figure 12. Plot of  $k_{ga}(a_H + K)^2(a_H + K_a)$  vs.  $a_H$  for the reaction of cysteamine with *m*-AMSA. The solid line is drawn through the least-squares-calculated points by using eq 23 with  $k_4'K^2K_a = 9.72 \times 10^{-27} \text{ M s}^{-1}$  and  $k_4K^2 + k_3'K_aK = 11.06 \times 10^{-18} \text{ s}^{-1}$ .

highest pH observed, and thus this made the  $k_4'K^2K_a$  term comparatively significant. Furthermore, at the lowest observed pH, the concentration of ionized cysteamine would be ~26%, which made the term  $(k_3K + k_5'K)a_H^2$

(12) (a) Bender, M. L.; Kezdy, F. J.; Zerner, B. *J. Am. Chem. Soc.* 1963, 85, 3017. (b) Capon, B.; Ghosh, B. C. *J. Chem. Soc. B* 1966, 472. (c) Fife, T. H.; DeMark, B. R. *J. Am. Chem. Soc.* 1979, 101, 7379.



+  $k_5 a_{\text{H}}^3$  negligible compared with the others in eq 16. Thus the observed data were found to follow eq 23. The

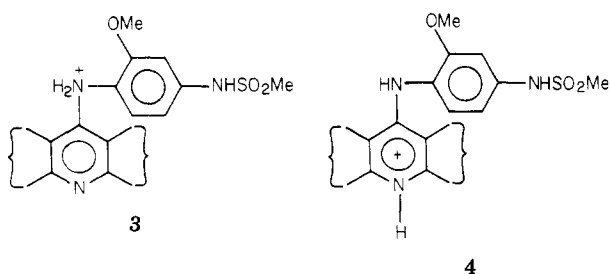
$$K_{\text{ag}}(a_{\text{H}} + K)^2(a_{\text{H}} + K_{\text{a}}) = k_4'K^2K_{\text{a}} + (k_4K^2 + k_3'K_{\text{a}}K)a_{\text{H}} \quad (23)$$

least-squares-calculated values of the intercept ( $k_4'K^2K_{\text{a}}$ ) and slope ( $k_4K^2 + k_3'K_{\text{a}}K$ ) were found to be  $(9.72 \pm 1.68) \times 10^{-27} \text{ M s}^{-1}$  and  $(11.06 \pm 0.28) \times 10^{-18} \text{ s}^{-1}$ , respectively. The  $k_4'$  calculated from the intercept and  $k_3'$  calculated from the slope (assuming  $k_3'K_{\text{a}}K \gg k_4K^2$ ) are summarized in Table II. Figure 12 indicates that the observed point at pH 7.78 is  $\sim 21\%$  positively deviated from linearity, which reveals the incursion of a significant contribution of the  $k_3$  and  $k_5$  terms.

(3) **Proposed Mechanism.** Wilson et al.<sup>13</sup> demonstrated that the nucleophilic thiolytic attack occurred at the C-9 position of *m*-AMSA in its in vivo as well as its in vitro degradation. The chain of *m*-AMSA was liberated as 4-amino-3-methoxymethanesulfonanilide (1). We also observed, in a study<sup>4</sup> oriented to product characterization, that it was the thiol group of both mono- and bifunctional thiols which reacted first, with the formation of the corresponding thioether 2. Thus the thiolytic cleavage of *m*-AMSA may be represented as



The kinetic studies revealed that the conversion of *m*-AMSA to 2 followed both nucleophilic and general-acid-catalyzed nucleophilic processes. The general-acid-catalyzed nucleophilic attack of thiol anions had not been observed in various previous studies<sup>14</sup> involving both soft and hard electrophiles. However, Sander et al.<sup>15</sup> observed the general-acid-catalyzed 2-mercaptoethanol addition to 5-iodouracil. It is not clear from previous studies whether the protonated *m*-AMSA exists in the form 3 or 4. The



(13) Wilson, W. R.; Cain, B. F.; Baguley, B. C. *Chem.-Biol. Interact.* 1977, 18, 163.

(14) (a) Friedman, M.; Cavins, J. F.; Wall, J. S. *J. Am. Chem. Soc.* 1965, 87, 3672. (b) Ogilvie, J. W.; Tildon, J. T.; Strauch, B. S. *Biochemistry* 1964, 3, 754. (c) Pohl, E. R.; Wu, D.; Hupe, D. J. *J. Am. Chem. Soc.* 1980, 102, 2759.

(15) Sedor, F. A.; Jacobson, D. G.; Sander, E. G. *Bioorg. Chem.* 1974, 3, 154.

(16) Pohl, E. R.; Hupe, D. J. *J. Am. Chem. Soc.* 1980, 102, 2763.

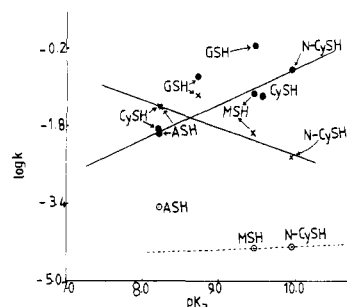
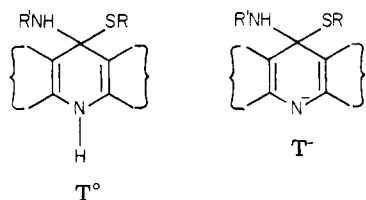


**Figure 13.** Brønsted plots for nucleophilic as well as general-acid-catalyzed thiolytic cleavage of *m*-AMSA at 30 °C: (a) nucleophilic bimolecular rate constants  $k_1'$  (○) for reaction between thiol anions and *m*-AMSA (free base) and  $k_1$  (●) for reaction between thiol anions and 4; (b) general-acid-catalyzed rate constants (×)  $k_3'$  for *N*-CySH, MSH, and ASH and  $k_5'$  for CySH and GSH. The solid line is drawn through the least-squares-calculated points by using  $\log k_1 = C_1 + \beta_{\text{nuc}} pK_{\text{a}}$  with  $C_1 = -8.03 \text{ M}^{-1} \text{ s}^{-1}$  and  $\beta_{\text{nuc}} = 0.74$  (●) and by using eq 24 with  $C_2 = 3.30 \text{ M}^{-2} \text{ s}^{-1}$  and  $\alpha_1 = 0.57$  (×). The observed points corresponding to GSH were excluded in the least-squares treatment for both ● and ×. The abbreviations GSH, CySH, *N*-CySH, MSH, and ASH represent glutathione, L-cysteine, *N*-acetylcysteine, 2-mercaptoethanol, and cysteamine, respectively. The broken line is drawn through only two observed points.

observed general-acid catalysis, however, indicates that probably 4 is the more likely protonated form of *m*-AMSA. The analysis of the limited number of kinetic data described in this manuscript led us to propose the mechanism in Schemes II and II for the thiolytic cleavage of *m*-AMSA. Scheme II is assumed to be operative if nucleophilic attack is the rate-determining step while scheme III is assumed to be taking place if expulsion of the leaving group is the rate-determining step. The present data are not very conclusive in differentiating these two kinetically indistinguishable mechanisms, and, in fact, the results are even insufficient to support without uncertainty the stepwise thiolytic process as compared with a concerted one.

The Brønsted plots for various nucleophilic and general-acid-catalyzed rate constants are shown in Figure 13. A plot of  $\log k_1$  vs.  $pK_{\text{a}}$  was found to be linear with slope  $\beta_{\text{nuc}} = 0.74 \pm 0.07$  and intercept  $C_1 = -8.03 \pm 0.68 \text{ M}^{-1} \text{ s}^{-1}$  where  $k_1$  is the bimolecular rate constant for reaction between  $\text{RS}^-$  and 4. The observed  $k_1$  values corresponding to both microscopic ionization constants of glutathione were found to be nearly 10 times larger than the ones expected from the Brønsted plot. An intramolecular general-acid catalysis for such deviations may be ruled out due to the fact that under such circumstances an enhanced reactivity cannot be expected for a nucleophile carrying no acidic proton; i.e.,  $k_2$ , in case of glutathione should fall on the Brønsted plot. At present we could only suggest that possibly the reactive site of glutathione constitutes another Brønsted plot of nearly similar  $\beta_{\text{nuc}}$  but values with a different intercept. The plot of  $\log k_1'$  vs.  $pK_{\text{a}}$  for *N*-acetylcysteine, 2-mercaptoethanol, and cysteamine is not linear (Figure 13). The reason for this could be the high standard deviations associated with these rate constants (Table II). However, a straight line passing through the points for *N*-acetylcysteine and 2-mercaptoethanol gave  $\beta_{\text{nuc}}' \approx 0.07$ , and then the observed point for cysteamine was found to be nearly 8 times higher than the calculated one. If  $\beta_{\text{nuc}}' \approx 0.07$  is really correct, then the positive deviation of cysteamine may be attributed to its probably intramolecularly general-acid-catalyzing power. Such a type of intramolecular general-acid catalysis was not observed in the nucleophilic thiolytic cleavage of 4 simply because of the difference in mechanism of thiolysis of 4 and *m*-AMSA. The ratios  $k_1/k_1'$  which give the measure

of the reactivity of 4 over *m*-AMSA were found to be on the order of  $10^3$  for simple thiols like *N*-acetylcysteine and 2-mercaptoethanol. These observations may be explained if we consider the relative stability of the reactive intermediates  $T^\circ$  and  $T^-$  involved in an assumed stepwise thiolytic process.

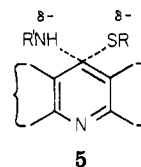


One may expect, by examining the eq 5 and 14, that the rate constants  $k_5'$  for L-cysteine and glutathione and  $k_3'$  for cysteamine, *N*-acetylcysteine, and 2-mercaptoethanol should fall on the same Brønsted line. These rate constants as shown in Figure 13 were found to follow eq 24

$$\log k_5'^3 = C_2 - \alpha_1 pK_a \quad (24)$$

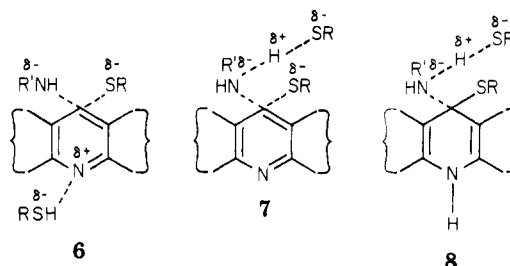
with exception of the rate constant for glutathione which, as usual, deviated positively from the plot. The least-squares-calculated values of  $C_2$  and  $\alpha_1$  are  $3.30 \pm 0.64 \text{ M}^{-2} \text{ s}^{-1}$  and  $0.57 \pm 0.07$ , respectively. It has been observed in various acyl-transfer reactions<sup>15</sup> that the dependence of the rate of thiolysis on the basicity of the nucleophiles is affected by the acidity of the leaving groups. Thus for a leaving group having a  $pK_a$  lower than that of the nucleophiles, the nucleophilic attack is the rate determining-step, with  $\beta_{\text{nuc}} = 0.27$ , and the breakdown of the tetrahedral intermediate has been demonstrated to be the rate-determining step with  $\beta_{\text{nuc}} = 0.87$  when the  $pK_a$  of the leaving group is higher than those of nucleophiles. The value of  $\beta_{\text{nuc}}$  is equal to 0.4 for the reactions of thiol anions with acrylonitrile<sup>14a</sup> and ethylene oxide,<sup>17</sup> and even smaller sensitivity to basicity has been reported<sup>18</sup> for the reaction of thiol anions with nonprotonated species of malachite green ( $\beta_{\text{nuc}} = 0.3$ ). Recently, Szajewski and Whitesides<sup>19</sup> reported a value of  $\beta_{\text{nuc}} \approx 0.5$  for the reduction of oxidized glutathione by thiol anions. A value of  $\beta_{\text{nuc}} = 0.38$ , obtained<sup>14b</sup> in the thiolytic cleavage of *p*-nitrophenyl acetate with nucleophiles of  $pK_a$  higher than that of *p*-nitrophenol, is close to the 0.27 value observed for the reactions where nucleophilic attack has been believed to be the rate-determining step. A significantly high value of  $\beta_{\text{nuc}}$  (0.74) indicates that a large amount of charge density from nucleophile has been transferred to the electrophilic center in the late transition state along the reaction coordinate. Thus the high sensitivity of the rate of thiolytic cleavage of 4 to the basicity of nucleophiles reveals that the expulsion of the leaving group is possibly the rate-determining step, which is conceivable due to the fact that the  $pK_a$  of the leaving group in 4 is much higher than those of thiols used as nucleophiles. The extremely weak sensitivity of the rate of thiolysis of *m*-AMSA to the basicity of nucleophiles ( $\beta_{\text{nuc}}' \approx 0.07$ ) indicates very little bond formation between the nucleophiles and the electrophilic center in the early transition state. This shows that the nucleophilic attack should be the rate-determining step in a stepwise mechanism, which is unlikely for the reason that the basicity of the leaving group is much higher than those of the nucleophiles. An alternative possibility to

explain the low value of  $\beta_{\text{nuc}}' (\approx 0.07)$  is that thiolysis of *m*-AMSA might be taking place via a concerted mechanism rather than a stepwise mechanism, and the concerted mechanism may involve an early transition state of the type 5 for which the driving force is probably the avoidance



of the formation of unstable intermediate  $T^-$  and the change in the coplanarity of the central ring due to the loss of its resonance character which would otherwise involve in a stepwise mechanism.

The general-acid-catalyzed nucleophilic thiolysis of *m*-AMSA is quite sensitive to the acidity of catalysts ( $\alpha_1 = 0.57$ ). This observation indicates that possibly a concerted general-acid-catalyzed thiolysis occurs via a transition states of the type 6 or 7. This assumption is based



on an elegant conclusion drawn by Jencks in a recent review<sup>20</sup> on how a change in the  $\alpha$  value could demonstrate the change of a mechanism from a stepwise to a concerted one. A stepwise mechanism for thiolysis of 4 could be justified due to the comparatively high stability of  $T^\circ$  and high value of  $\beta_{\text{nuc}}$  (0.74).

**Acknowledgment.** This research was supported by a grant from the National Cancer Institute.

## Appendix

### I. By definition

$$A = k_2 K_C K_A + k_1' K_a K_A + k_3' K_B K_A \quad (i)$$

But, under the experimental conditions,  $k_3' K_B K_A$  should be negligible in comparison to  $k_2 K_C K_A + k_1' K_a K_A$ , and thus the application of this assumption reduces eq i to eq ii.

$$A = k_2 K_C K_A + k_1' K_a K_A \quad (ii)$$

The value of  $k_1'/k_2$  could be estimated as in eq iii. In eq

$$\frac{k_1'}{k_2} = \frac{k_1' k_1}{k_1 k_2} \approx 0.033 \times 0.10 \approx 3.3 \times 10^{-3} \quad (iii)$$

iii, the value of  $k_1'/k_1 (\approx 0.033)$  was obtained from the analysis of the observed data for cysteaminolysis of *m*-AMSA by assuming that the ratio ( $k_1'/k_1$ ) would be nearly the same for both cysteaminolysis and cysteinolysis of *m*-AMSA under essentially similar conditions. The value of  $k_1/k_2 (\approx 0.10)$  was obtained by assuming that  $k_1$  and  $k_2$  would fall on a Brønsted plot of  $\beta_{\text{nuc}} = 0.74$ .

On calculation of  $k_1'/k_2$  for glutathionolysis of *m*-AMSA, the value of  $k_1'/k_1$  was estimated as  $1.73 \times 10^{-3}$  by assuming  $k_1'$  and  $k_1$  would fall on Brønsted plots of  $\beta = 0.07$  and 0.74, respectively. Similarly,  $k_1/k_2$  was estimated to be 0.10 by assuming  $\beta = 0.74$ .

(17) Deneby, J. P.; Noel, C. J. *J. Am. Chem. Soc.* 1960, 82, 2511.

(18) Reuben, D. M. E.; Bruice, T. C. *J. Am. Chem. Soc.* 1976, 98, 114.

(19) Szajewski, R. P.; Whitesides, G. M. *J. Am. Chem. Soc.* 1980, 102, 2011.

(20) Jencks, W. P. *Acc. Chem. Res.* 1980, 13, 161.

## II. By definition

$$D = (k_6'K_A + k_9'K_B + k_8K_C)K_BK_A + k_7'K_CK_AK_A \simeq \frac{k_6'K_AK_BK_A + k_7'K_CK_AK_A}{k_6'K_AK_BK_A + k_7'K_CK_AK_A} \quad (\text{iv})$$

for it can be shown by an approximate estimation that  $(k_9'K_B + k_8K_C)K_BK_A$  will not contribute more than ~4% to the observed value of  $D$ . The lower limit of the obtained  $\alpha$  (0.50) was used in the estimation of  $k_6'$  and  $k_7'$ .

The calculation of  $k_6'$  from  $E$  was carried out as in eq v because an approximate estimate has revealed that the

$$E = \frac{(k_6K_A + k_9K_B)K_B + (k_5'K_A + k_7K_C)K_A}{(k_6K_A + k_9K_B)K_B + (k_5'K_A + k_7K_C)K_A} \text{ or } E \simeq \frac{k_5'K_AK_A}{(k_6K_A + k_9K_B)K_B + (k_5'K_A + k_7K_C)K_A} \quad (\text{v})$$

contribution due to  $(k_6K_A + k_9K_B)K_B + k_7K_CK_A$  to  $E$  should not be more than ~3.5%. Equation v was used for calculation of  $k_5'$ .

**Registry No.** *m*-AMSA, 51264-14-3; L-cysteine, 52-90-4; glutathione, 70-18-8; *N*-acetylcysteine, 616-91-1; 2-mercaptoethanol, 60-24-2; cysteamine, 60-23-1.

## Reactivity of Geometrically Constrained Cyclopropylcarbinyl and Homoallyl Substrates. Solvolysis of 2,4-Dehydro-5-homoadamantyl and 2-Homoadamant-4-enyl Derivatives

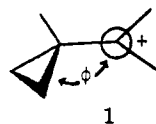
J. Milton Harris,\*<sup>1</sup> John R. Moffatt,<sup>1</sup> Martha G. Case,<sup>1</sup> Frederick W. Clarke,<sup>1</sup> Judith S. Polley,<sup>2</sup> Thomas K. Morgan, Jr.,<sup>2</sup> Thomas M. Ford,<sup>2</sup> and Roger K. Murray, Jr.\*<sup>2,3</sup>

<sup>1</sup>Departments of Chemistry, The University of Alabama in Huntsville, Huntsville, Alabama 35899, and  
<sup>2</sup>University of Delaware, Newark, Delaware 19711

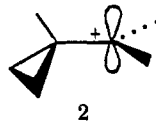
Received February 4, 1982

Solvolysis of 5-*endo*-2,4-dehydrohomoadamantyl 3,5-dinitrobenzoate (5) or 2-*exo*-chloro-4-homoadamantene (6) in buffered 70% aqueous acetone gives a very similar mixture of products by way of an apparent common intermediate. The formation of 5-*endo*-hydroxy-2,4-dehydrohomoadamantane as the major reaction product suggests that this species is a nonplanar 2,4-dehydro-5-homoadamantyl cation. When compared to the kinetic behavior of structurally analogous derivatives which react with unassisted ionization, both 5 and 6 show large solvolytic rate enhancements. The unusually large acceleration for 6 seems to be a consequence of the particular stereoelectronic arrangement of the double bond and the leaving group in this compound. In contrast to these results, 2-*endo*-homoadamant-4-enyl tosylate (7) solvolyzes 11 times more slowly than its saturated analogue to give a mixture of 2-*endo*- and 2-*exo*-hydroxyhomoadamant-4-ene. Since the solvolysis of 7 occurs by a  $k_c$  process, this may provide the best available measure of the inductive destabilization of a cationic center by a homoallylic double bond.

The rapid interconversion of cyclopropylcarbinyl, cyclobutyl, and homoallyl derivatives in solvolytic systems has attracted considerable attention.<sup>4</sup> As a result of both experimental studies and theoretical calculations, it is clear that the "bisected" conformation (1) of a cyclopropyl-



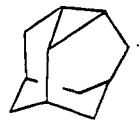
1



2

carbinyl cation is significantly energetically favored over the "perpendicular" conformation (2).<sup>4</sup> Recently, it has been demonstrated that a cyclopropylcarbinyl cation is also stabilized when the conformation of the system is locked by structural constraints at an intermediate position between bisected and perpendicular.<sup>5</sup> Indeed, the change in energy of a cyclopropylcarbinyl cation upon rotation of

the cation center seems to follow a function that is very similar to a  $\cos^2 \phi$  relationship (with  $\phi$  being the angle of rotation).<sup>5</sup> In view of these observations, we were interested in examining the solvolytic generation of the 2,4-dehydro-5-homoadamantyl cation (3) and comparing its



3



4

behavior with that of the 8,9-dehydro-2-adamantyl cation (4) which is constrained to the bisected conformation ( $\phi = 0^\circ$ ). If the solvolysis of 2-adamantyl tosylate is used as a model for the localized cation 4, then the rate enhancement associated with the assisted formation of a cation from 8,9-dehydro-2-adamantyl tosylate in acetolysis at 25 °C is  $2.5 \times 10^8$ .<sup>6</sup> An examination of Dreiding molecular models shows that for such an idealized representation of 3 the dihedral angle  $\phi$  between the axis of the vacant p orbital at C-5 and the adjacent cyclopropyl moiety should be about 30°. Thus, it can be anticipated that ion 3 will experience only some of the cyclopropyl stabilization effective in 4.

Ions 3 and 4 have been studied previously under stable ion conditions by NMR spectroscopy.<sup>7,8</sup> Ion 3 is static at

(1) University of Alabama in Huntsville.

(2) University of Delaware.

(3) Recipient of a Camille and Henry Dreyfus Teacher-Scholar Grant Award, 1976-1981.

(4) For reviews see: (a) Wiberg, K. B.; Hess, B. A., Jr.; Ashe, A. J., III "Carbonium Ions", Olah, G. A., Schleyer, P. v. R., Eds.; Wiley-Interscience: New York, 1972; Vol. III, Chapter 26. (b) Richey, G. *Ibid.* Chapter 25. (c) Story, P. R.; Clark, P. R., Jr. *Ibid.* Chapter 23. (d) Haywood-Farmer, J. *Chem. Rev.* 1974, 74, 315-350. (e) Brown, H. C. "The Non-classical Ion Problem", Plenum Press: New York, 1977; Chapter 5.

(5) de Meijere, A.; Schallner, O.; Weitemeyer, C. *Angew. Chem., Int. Ed. Engl.* 1972, 84, 56-57. Rhodes, Y. E.; DiFate, V. G. *J. Am. Chem. Soc.* 1972, 94, 7582-7583. Andersen, B.; Schallner, O.; de Meijere, A. *Ibid.* 1975, 97, 3521-3522. de Meijere, A.; Schallner, O.; Weitemeyer, C.; Spielmann, W. *Chem. Ber.* 1979, 112, 908-935.

(6) Baldwin, J. E.; Foglesong, W. D. *J. Am. Chem. Soc.* 1968, 90, 4303-4310.